Photorespiration Is Crucial for Dynamic Response of Photosynthetic Metabolism and Stomatal Movement to Altered CO_2 Availability

Marion Eisenhut[1], Andrea Bräutigam[1,4], Stefan Timm[2], Alexandra Florian[3], Takayuki Tohge[3], Alisdair R. Fernie[3], Hermann Bauwe[2] and Andreas P.M. Weber[1,*]

[1]Institute of Plant Biochemistry, Cluster of Excellence on Plant Sciences, Heinrich Heine University, 40225 Düsseldorf, Germany

[2]Department of Plant Physiology, University of Rostock, Albert-Einstein-Straße 3, 18051 Rostock, Germany

[3]Department of Molecular Physiology, Max-Planck Institute for Molecular Plant Physiology, 14476 Potsdam-Golm, Germany

[4]Present address: IPK Gatersleben, Network Analysis and Modeling, Corrensstrasse 3, 06466 Seeland, Germany

*Correspondence: Andreas P.M. Weber (andreas.weber@uni-duesseldorf.de)

http://dx.doi.org/10.1016/j.molp.2016.09.011

ABSTRACT

The photorespiratory pathway or photorespiration is an essential process in oxygenic photosynthetic organisms, which can reduce the efficiency of photosynthetic carbon assimilation and is hence frequently considered as a wasteful process. By comparing the response of the wild-type plants and mutants impaired in photorespiration to a shift in ambient CO_2 concentrations, we demonstrate that photorespiration also plays a beneficial role during short-term acclimation to reduced CO_2 availability. The wild-type plants responded with few differentially expressed genes, mostly involved in drought stress, which is likely a consequence of enhanced opening of stomata and concomitant water loss upon a shift toward low CO_2. In contrast, mutants with impaired activity of photorespiratory enzymes were highly stressed and not able to adjust stomatal conductance to reduced external CO_2 availability. The transcriptional response of mutant plants was congruent, indicating a general reprogramming to deal with the consequences of reduced CO_2 availability, signaled by enhanced oxygenation of ribulose-1,5-bisphosphate and amplified by the artificially impaired photorespiratory metabolism. Central in this reprogramming was the pronounced reallocation of resources from growth processes to stress responses. Taken together, our results indicate that unrestricted photorespiratory metabolism is a prerequisite for rapid physiological acclimation to a reduction in CO_2 availability.

Key words: photorespiration, starvation, stress, stomata, transcription, *Arabidopsis thaliana*

INTRODUCTION

Life on Earth relies on carbon. Carbon moves through several reservoirs in the atmosphere and the oceans both in organic and inorganic forms, with the processes of photosynthesis and respiration accounting for the majority of the global carbon cycle (Falkowski et al., 2000). Photosynthetic organisms play a central role in carbon cycling, as they are able to transform atmospheric inorganic carbon dioxide (CO_2) into organic carbon in the form of sugar phosphates. Central to this process is the enzyme ribulose-1,5-bisphosphate carboxylase/oxygenase (Rubisco). When Rubisco evolved approximately 3 billion years ago, the enzyme operated at high CO_2 concentrations whereas oxygen (O_2) concentrations were negligible (Nisbet et al., 2007). Once the O_2

concentration in the cell, and later in the air, increased as a consequence of oxygenic photosynthesis, the oxygenation side reaction of Rubisco produced the dead-end metabolite 2-phosphoglycolate (2PG), sequestering a significant fraction of phosphate and carbon from the Calvin-Benson-Bassham (CBB) cycle metabolite pool. Consequently, a salvage pathway evolved that in plants and most algae comprises a series of nine consecutive enzymatic steps that are distributed between chloroplasts, peroxisomes, mitochondria, and the cytosol. This photorespiratory (PR) pathway not only removes harmful intermediates but

also returns the bound phosphate and three out of four carbon atoms contained in two molecules each of 2PG to the CBB cycle, while one carbon atom is lost as CO_2 (reviewed in Somerville, 2001; Bauwe et al., 2012). Therefore, PR metabolism is of vital importance for all oxygenic photosynthetic organisms (Eisenhut et al., 2008; Bauwe et al., 2012), as documented by the observation that cyanobacterial, green algal, and plant mutants in this pathway can only survive in an atmosphere with elevated CO_2 levels (Somerville and Ogren, 1979; Somerville, 2001; Nakamura et al., 2005; Voll et al., 2006; Engel et al., 2007; Schwarte and Bauwe, 2007; Eisenhut et al., 2008; Timm et al., 2011). Besides its metabolic repair function in the removal of the Rubisco's oxygenation product 2PG and carbon salvage, PR metabolism has also been suggested to protect from photoinhibition (Heber and Krause, 1980; Osmond, 1981; Kozaki and Takeba, 1996; Takahashi et al., 2007; Voss et al., 2013). PR is crucial for maintaining the activity of the CBB cycle, since it prevents both the accumulation of enzyme-inhibiting metabolites (Anderson, 1971; Kelly and Latzko, 1976; Norman and Colman, 1991) and the depletion of intermediates from the CBB cycle. PR contributes to a steady consumption of reducing equivalents by the operation of the CBB cycle, and by this reduces acceptor limitation and generation of harmful reactive oxygen species (ROS) under highlight conditions (Takahashi and Badger, 2011). However, whether the functions of PR extend beyond metabolic repair is still a matter of intense debate.

Here we tested the hypothesis that PR contributes to rapid acclimation to reduced CO_2 availability at the site of Rubisco. Homoiohydric land plants frequently experience episodes of leaf internal CO_2 limitation, for example when their stomata close to prevent dehydration. To test this hypothesis, we analyzed the physiological and transcriptomic response of wild-type (WT) and mutant *Arabidopsis thaliana* (*Arabidopsis*) plants, which had been cultivated at high CO_2 conditions (1% CO_2 in air) that repress PR, to a shift to ambient CO_2 conditions (0.038% CO_2 in air), which rapidly increase flux through the PR pathway (Szecowka et al., 2013). To distinguish between general effects of altered CO_2 availability from specific effects due to flux through the PR pathway, we included in our study mutants deficient in the PR pathway: phosphoglycolate phosphatase, *pglp1* (Schwarte and Bauwe, 2007), serine hydroxymethyltransferase, *shm1* (Voll et al., 2006), hydroxypyruvate reductase 1, *hpr1* (Timm et al., 2008), and glycerate kinase, *glyk1* (Boldt et al., 2005). These mutations affect enzyme activities required for PR in three different cellular compartments, chloroplasts (*pglp1*, *glyk1*), peroxisomes (*hpr1*), and mitochondria (*shm1*), and accumulate different PR intermediates. Comparing the responses in WT plants with those in PR mutants identified the safekeeping functions of PR, and also revealed the shared reprogramming as an emergency strategy of the mutants with full block in PR.

RESULTS

High-To-Low CO_2 Transition Induces PR and Results in Strong and Distinct Metabolic Changes in PR Mutants

To verify that reduction in external CO_2 availability enhances flux through the PR pathway, we comparatively analyzed *Arabidopsis* WT plants and four different PR mutant lines (Figure 1), *pglp1*,

shm1, *hpr1*, and *glyk1*. The *shm1*, *glyk1*, and *pglp1* mutants are categorized as "strong" mutants, since they display a photorespiratory phenotype in ambient air, including chlorotic leaves, stunted growth, or even lethality. The *hpr1* mutant shows only minor phenotypic alteration when grown in ambient air and is therefore categorized as a "weak" mutant (Timm et al., 2012; Timm and Bauwe, 2013). Under high CO_2 conditions all plant lines grow likewise. Only the *pglp1* mutant shows smaller rosettes (Timm et al., 2012). To avoid pre-term stress conditions and pleiotropic effects due to long-term effects of the mutations, we continuously grew the plants under high CO_2 (air enriched with 1% CO_2; HC) conditions that largely suppress PR, and then transferred the lines to ambient air (0.038% CO_2; LC) at the end of the dark period to induce PR in the following light period. We sampled plant material under both conditions 8 h after the onset of illumination for metabolite and transcript analysis, i.e., the analyzed mutants and WT had experienced PR conditions for only 8 h during their entire life cycle. The quantification of leaf metabolites revealed four significant changes in WT plants. The shift to LC led to significantly larger intracellular pools of glycolate, glycine, serine, and glycerate (Figure 1 and Supplemental Table 1), which are all central intermediates of the PR pathway. These metabolite pools remained elevated also 3 and 5 days after the shift to LC conditions (Supplemental Figure 1). The mutant plants accumulated metabolites characteristic for their mutations. In the *pglp1* mutant glycolate accumulation was detected, which is most likely a consequence of in-source dephosphorylation of 2PG during mass spectrometry (MS) analysis. The *shm1* mutant accumulated mainly glycine and had reduced serine levels. Metabolic consequences of the *hpr1* mutation were elevated levels of glycolate, serine, glycine, and glycerate compared with HC conditions. The *glyk1* mutant strongly accumulated glycerate and serine upon shift to LC conditions (Figure 1 and Supplemental Table 1).

In addition to the increase of PR metabolites, the *pglp1*, *shm1*, and *glyk1* mutants were also strongly affected in amino acid metabolism by the LC shift. The branched-chain amino acids valine and isoleucine, and the aromatic amino acids phenylalanine, tryptophan, and tyrosine increased in abundance. In contrast, the amounts of glutamate were significantly reduced. The WT, *hpr1*, *shm1*, and *glyk1* mutants furthermore showed significantly reduced alanine levels (Supplemental Table 1).

Photorespiratory Mutants Show Strong Transcriptional Responses to LC Shift

For assessment of the transcriptional changes in response to a short-term reduction of the external CO_2 concentration, three independent biological replicates of WT, and two independent biological replicates of *hpr1*, *shm1*, *glyk1*, and *pglp1* plants were sampled as stated above and subjected to RNA-sequencing (RNA-seq) analysis. A principal component analysis (PCA) identified the CO_2 availability as the major variable (43%) contributing to transcriptional variation. The genotype was the second variable, accounting for 20% of the variation (Figure 2A). As expected, all HC samples and also the LC samples of WT and the weak mutant *hpr1* clustered together, whereas LC samples of the strong mutants *shm1*, *glyk1*, and *pglp1* were distant.

In accordance with the PCA results, comparison of the genotype specific transcriptomes revealed vast differences in
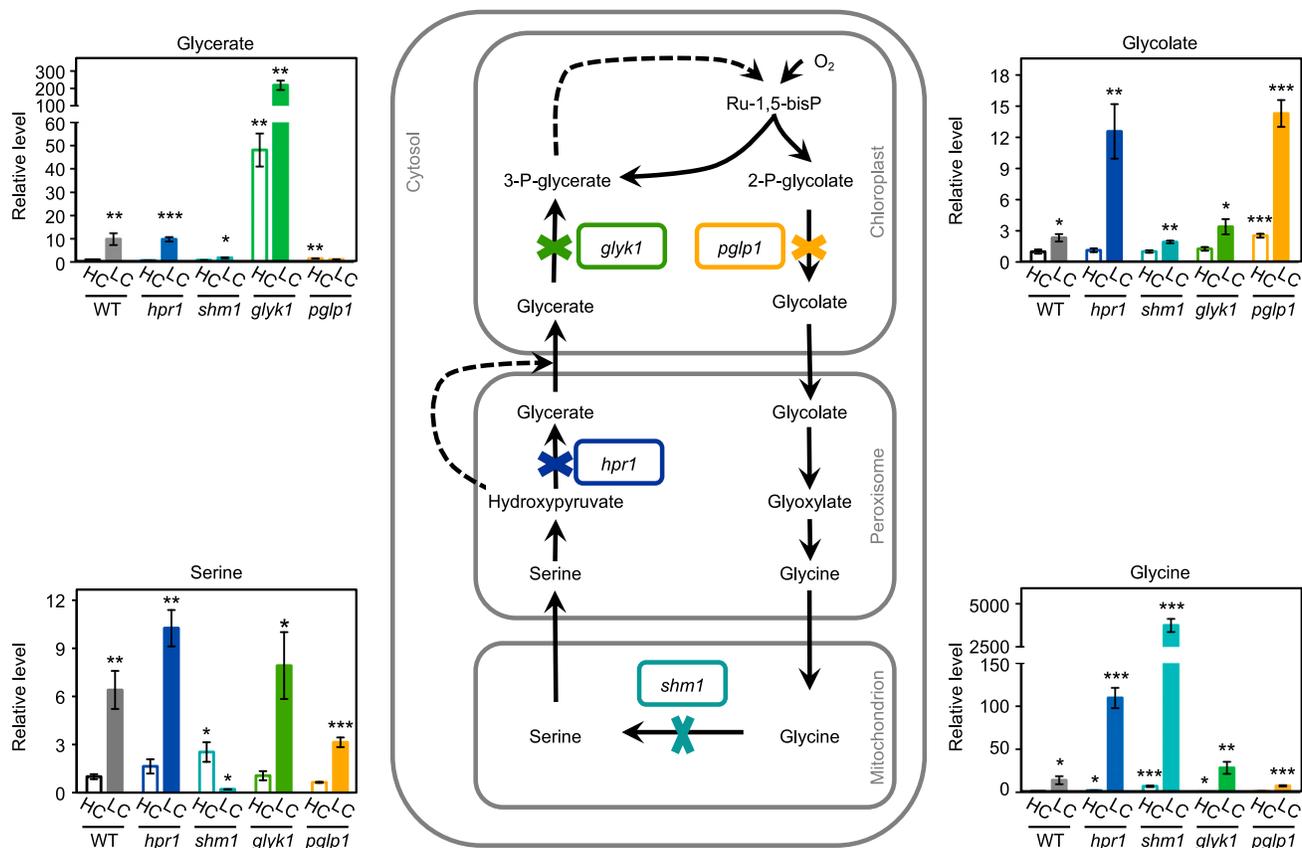
Figure 1. Simplified Presentation of the PR Pathway.

Mutants selected for this study are indicated and specifically colored. The color code is applied throughout this study. Relative changes in quantities of the PR metabolites glycolate, glycine, serine, and glycerate upon shift from HC to LC conditions are shown for WT and the mutant lines. Values were normalized to the concentration of the WT under HC conditions. Data are shown as means ± SE. Asterisks indicate significant changes (*$P < 0.05$, **$P < 0.01$, ***$P < 0.001$) to WT HC values.

the amount of significantly differentially expressed genes after the shift to LC. In WT plants we identified only five significant changes ($q < 0.01$, representing 0.02% of all genes), in *hpr1* 559 changes ($q < 0.01$; 2.0%), in *shm1* 6304 changes ($q < 0.01$; 22.1%), in *glyk1* 5064 changes ($q < 0.01$; 17.8%), and in *pglp1* 5944 changes ($q < 0.01$; 20.9%) between HC and LC conditions (Figure 2B). The response in WT and *hpr1*, which are both capable of completing the PR pathway, albeit with differing efficiency, was at least one order of magnitude smaller compared with the response in the strong mutants *shm1*, *glyk1*, and *pglp1*, which cannot complete the PR pathway. In these mutants both the number of changed transcripts and the amplitude of the change was large (Figure 2B).

The Nature of Transcriptional Response Depends on the Phenotype Severity

The transcriptional response of the WT was limited to five genes (Table 1). Four of the encoded proteins, leucoanthocyanidin dioxygenase (LDOX, TT18), dihydroflavonol 4-reductase (DFR, TT3), glutathione *S*-transferase phi 12 (GSTF12, TT19), and UDP-glucose:flavonoid 3-*O*-glucosyltransferase (Fd3GlcT, UF3GT) are involved in anthocyanin production, and TT3 and TT19 belong to the drought and abscisic acid (ABA)

regulated network (Huang et al., 2008). The fifth gene (*AT2G41800*) encodes a cell-wall protein of unknown function.

For the PR mutants the transcriptional response was larger. To assess the similarities and the differences between the transcriptional responses, we plotted shared and uniquely regulated genes using Venn diagrams (Supplemental Figure 2). The largest number of shared downregulated genes (750) was in the overlap between the strong mutants *shm1*, *glyk1*, and *pglp1*. In contrast, only 60 differentially downregulated genes were shared between all mutants (Supplemental Figure 2). The shared upregulated genes painted a similar picture. The largest number of shared upregulated genes was again in the overlap of the three strong mutants with 1443 genes. The number of shared upregulated genes between all mutants was 241 (Supplemental Figure 2). We could not detect any commonly regulated gene between all mutants and WT. In relation to the total number of differentially regulated genes in the PR mutants, the commonly regulated genes occupied a share of 40%–50%. In the case of *hpr1*, 54% of all differentially regulated genes were shared with all other mutants (Figure 3A), *shm1* shared 5% with all mutants and 35% with the other two strong mutants, *glyk1* shared 6% and 43%, and *pglp1* shared 5% and 37% of its differentially regulated genes with all and the strong mutants, respectively (Figure 3A). These results indicated that some transcriptional changes in PR
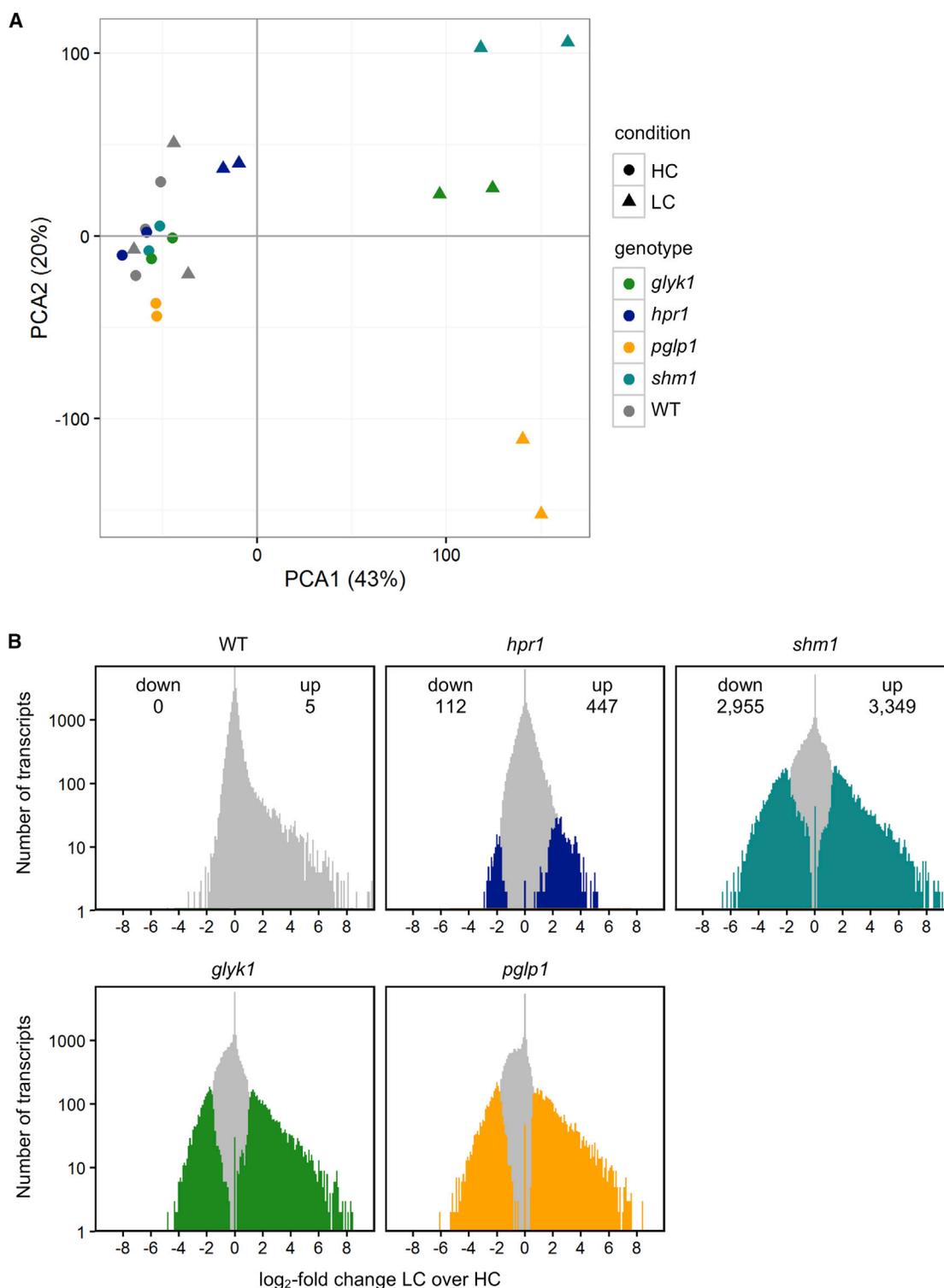
Figure 2. Effect of Shift from HC (1% CO_2 in Air) to LC (0.038% CO_2 in Air) Conditions on Transcriptomes of WT and PR Mutants.
RNA was isolated 8 h after shift to LC and onset of light and subjected to RNA-seq analysis.
(A) Principal component analysis of normalized transcriptome data. Dots represent HC samples and triangles LC samples.
(B) Comparison of global transcriptional response toward a shift from HC to LC conditions. All changes are given as log_2-fold values compared with HC. Gray represents insignificant changes, while significant changes ($q < 0.01$, edgeR, Robinson et al., 2010) are presented in color. The number of significantly up- and downregulated genes is given for each genotype.

Gene ID	Annotation (TAIR10)	LC/HC (log$_2$ fold)	q value
AT4G22880	Leucoanthocyanidin dioxygenase (LDOX, TT18)	6.34	0.00332
AT5G42800	Dihydroflavonol 4-reductase (DFR, TT3)	6.24	0.00969
AT5G17220	Glutathione *S*-transferase phi 12 (GSTF12) TRANSPARENT TESTA 19 (TT19)	5.56	0.00615
AT5G54060	UDP-glucose:flavonoid 3-*O*-glucosyltransferase (Fd3GlcT, UF3GT)	5.01	0.00553
AT2G41800	Unknown function	4.54	0.00223

Table 1. Differentially Regulated Genes in WT upon Shift from HC (1% CO$_2$) to LC (0.038% CO$_2$) Conditions.
Changes are given as log$_2$-fold values compared with HC. The *q* value was calculated with edgeR (Robinson et al., 2010). Drought/ABA regulated genes (according to Huang et al., 2008) are written in bold.

mutants followed a minor common pattern in all mutants and that the shared pattern in the strong mutants *shm1*, *glyk1*, and *pglp1* was more pronounced.

To identify and further study these patterns, we analyzed gene ontology (GO) terms. The comparison of shared enriched GO terms provides a sense of the biological pathways, which are commonly up- or downregulated. GO term enrichments were calculated for each mutant as HC-LC significantly up- and down-regulated gene set in contrast with all gene models, respectively (Supplemental Table 2). All mutants shared GO terms of single-organism cellular and biosynthetic processes, cellular component biogenesis, and polysaccharide metabolic process among the downregulated genes (four terms in total, Figure 3B) and shared GO terms related to response terms to stress, water, and endogenous stimulus among the upregulated terms (seven terms in total, Figure 3C). The strong mutants *shm1*, *glyk1*, and *pglp1* shared starch, sulfur, and phosphorous metabolism, and isopentenyl pyrophosphate (IPP) biosynthesis among the GO terms of downregulated genes (nine in total, Figure 3B). Among the shared upregulated terms (75 in total, Figure 3C), the categories protein folding and targeting, responses to ABA, jasmonate (JA), and salicylic acid, innate immunity, respiratory burst, and terms related to cell death were covered. Each of the mutants also showed a large number of unshared GO terms (51, 47, 2, and 11 for unique among downregulated GO terms and 0, 7, 0, and 2 for unique among upregulated GO terms) (Figure 3B and 3C; Supplemental Table 2).

Besides the GO term analysis, the top 50 of shared down- and upregulated genes were also inspected (Supplemental Table 3). Among the upregulated genes a remarkably high number of genes encoded UDP-glucosyltransferases (10 in all mutants and 2 in strong mutants), and glutathione *S*-transferases and proteins of the thioredoxin system, respectively (five and eight). Among the most downregulated genes shared between the strong mutants, we identified eight genes involved in the biosynthesis and binding of chlorophyll (Supplemental Table 3). The top-50 lists additionally allowed searching for transcription factors that were potentially mediating the transcriptional response of the PR mutants toward the shift in CO$_2$ concentrations. Among the upregulated genes, four transcriptional regulators were shared between all mutants (Table 2; RAP2.6, ABR1, AT1G10585, AT1G71520) and another four were shared between the strong mutants *shm1*, *glyk1*, and *pglp1* (Table 2; WRKY40, WRKY 75, DIN11, AT3G46080). Among the most downregulated genes shared between the strong mutants two

transcription factors were detected (Table 2; HBI1 and BZIP61). The majority of these transcriptional regulators, RAP2.6, ABR1, AT1G10585, AT1G71520, and WRKY40, were characterized as being involved in the response to drought stress and ABA (Pandey et al., 2005; Chen et al., 2010; Zhu et al., 2010; Ding et al., 2013). In all strong mutants the transcripts of DIN11 and WRKY75 were induced, both of which are involved in starvation responses. DIN11 is central in gene regulation during sugar starvation (Fujiki et al., 2001) and WRKY75 plays a role in Pi starvation (Devaiah et al., 2007).

In conclusion, the analysis of the transcriptomes indicated a very limited transcriptional response of the WT but a general stress response in all PR mutants toward the reduction in CO$_2$ availability. The range and power of the transcriptional response correlated with the strength of the mutants' phenotype.

General Transcriptional LC Response Overlaps Significantly with Drought Stress Response

The presence of stress-related GO terms in the overlap between all mutants, in particular with regard to ABA and drought, prompted a closer investigation. Work on stomatal opening and closing mechanisms (Hu et al., 2010; Xue et al., 2011; Tian et al., 2015) predicted stomatal opening upon reduced external CO$_2$ concentration. Using the apparent transpiration rates as a proxy for stomatal aperture, WT and *hpr1* plants indeed showed the expected short-term response, i.e., stomatal opening. Specifically, 1 day after the shift from HC to LC the transpiration rate was two-fold higher in WT and *hpr1*. However, the strong PR mutants *shm1*, *glyk1*, and *pglp1* showed the opposite response, with open stomata under HC conditions and closed stomata upon LC shift. The transpiration rate returned to pre-shift conditions over the course of 5 days in the WT and *hpr1*. In the strong PR mutants, the transpiration rate remained stable compared with day 1 of the shift (Figure 4A).

Concomitant with the GO term analyses, the transcriptome of all plant lines showed significant changes (*q* < 0.01) consistent with a response of water stress. The LC transcriptome datasets overlapped significantly (*P* < 0.05) with transcriptome data obtained from plants that were challenged with drought stress or treated with ABA (Huang et al., 2008). Of the five differentially regulated genes of the WT LC transcriptome, two genes (40%) belonged to the set of ABA-responsive genes (Supplemental Table 4). The *hpr1* mutant's transcriptome contained 80 (14.3% of all significantly regulated genes)
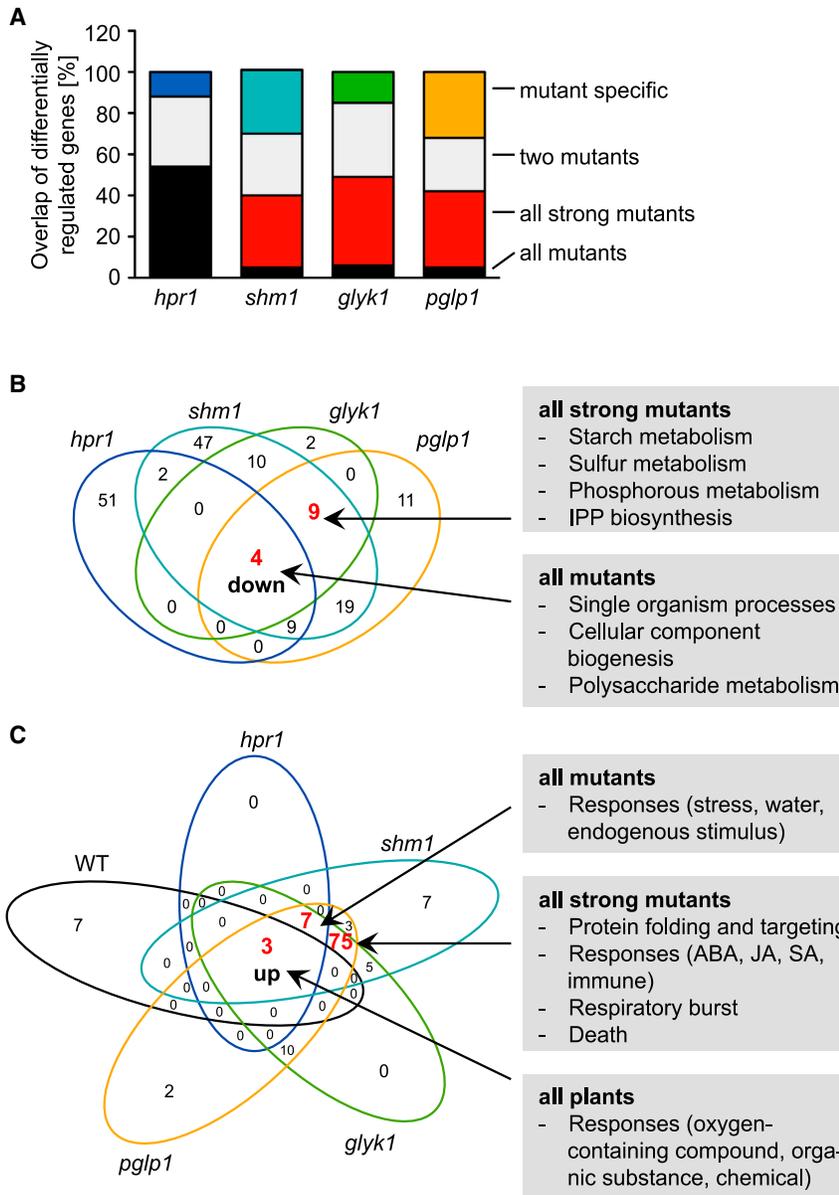
Figure 3. Overlap in Transcriptional Responses of PR Mutants upon Shift from HC to LC Conditions.

(A) Overlap of differentially regulated genes between PR mutants. Presented are shares (in %) for overlap between all mutants, all strong mutants, two mutants, and mutant-specific responses. The total number of differentially regulated genes per genotype was set to 100% and the percentage of shared genes calculated from the numbers given in Supplemental Figure 1.

(B and C) Comparison of shared, significantly enriched GO terms. Results of the qualitative assessment of GO terms of downregulated gene sets **(B)** and upregulated gene sets **(C)** were plotted as Venn diagrams. Numbers of shared and unique GO terms, respectively, are indicated. Red numbers indicate the count of shared GO terms between all plants (WT, *hpr1*, *shm1*, *glyk1*, *pglp1*), all mutants (*hpr1*, *shm1*, *glyk1*, *pglp1*), or all strong mutants (*shm1*, *glyk1*, *pglp1*). Enriched GO terms of downregulated **(B)** or upregulated **(C)** gene sets shared by all plants, all mutants, or all strong mutants are listed in gray boxes. Significant enrichment ($q < 0.01$) was tested using TopGO (Alexa and Rahnenfuhrer, 2010).

To better understand the abnormal transpiration pattern in *shm1*, *glyk1*, *and pglp1*, we inspected the regulatory elements in stomatal aperture and also extended the analysis to the light-dependent regulatory pathways. While most components were not significantly changed in transcription, we found in the strong mutants significantly elevated transcript abundances for the protein phosphatases ABI1 and ABI2 (Figure 4C), which function as negative regulators in the ABA-signaling pathway (Merlot et al., 2001). Additionally, the two respiratory burst oxidase proteins, RBOHD and RBOHF, were strongly induced in expression after the shift to LC conditions in *glyk1* and *pglp1* (Figure 4D). In *shm1* only the expression of RBOHD was upregulated (Figure 4D). These proteins generate ROS in guard cells and thus induce stomatal closure (Kwak et al., 2003), which is also a central part of the innate immune response (Göhre et al., 2012). Stomatal opening is essentially induced by light (Shimazaki et al., 2007). Blue light (BL) and photosynthetic active radiation stimulate two parallel, specific signaling pathways (reviewed in Kollist et al., 2014). BL is sensed by the phototropins PHOT1 and PHOT2 (Kinoshita et al., 2001) and induces H^+-ATPases, while inhibiting anion channels in guard cell membranes (Marten et al., 2010). Thereby, BL provokes opening of the pore. All plant lines expressed *PHOT1* and *PHOT2* at the same levels under HC conditions (Figure 4E). After the LC shift we did not observe for WT and *hpr1* mutant any changes in expression of these genes. However, in the strong mutants *shm1*, *glyk1*, and *pglp1*, *PHOT1* was significantly reduced in transcript abundance by 80%–95%. In *shm1* and *glyk1*,

ABA-responsive genes, the *shm1* mutant's transcriptome 420 (6.7%), the *glyk1* mutant's transcriptome 278 (5.5%), and the *pglp1* mutant's transcriptome 419 (7.0%, Supplemental Table 4).

In agreement with the transcriptional ABA response, we detected a significant 2.5-fold increase of ABA in leaves of the WT after LC shift (Figure 4B). The transpiration rate returned to normal within 5 days (Figure 4A), as did the transcriptional response after a shift from HC to LC conditions (Queval et al., 2012). In mutant plants, *glyk1* and *pglp1* showed likewise significant ABA accumulation, and *hpr1* and *shm1* displayed a non-significant trend toward ABA accumulation (Figure 4B). The strong mutants' stomatal opening, however, showed different openness compared with the weak mutant *hpr1* and WT. Transpiration rates were actually higher under HC conditions and decreased under LC conditions, which was the reverse type of regulation compared with WT and *hpr1*, where transpiration rates increased during shift (Figure 4A).

Gene ID	Annotation (TAIR10)	Condition	Reference
Upregulated all mutants			
AT1G10585	Basic helix-loop-helix DNA-binding superfamily protein	Dehydration stress memory	Ding et al., 2013
AT1G43160	Member of the ERF (ethylene response factor) subfamily B-4 of ERF/AP2 transcription factor family (RAP2.6)	Response to ABA, high salt, osmotic stress, cold	Zhu et al., 2010
AT1G71520	Member of the DREB subfamily A-5 of ERF/AP2 transcription factor family	Dehydration stress memory	Ding et al., 2013
AT5G64750	ABA REPRESSOR1 (ABR1)	Response to ABA, osmotic stress, sugar stress, drought	Pandey et al., 2005; Ding et al., 2013
Upregulated all strong mutants			
AT1G80840	WRKY DNA-BINDING PROTEIN 40 (WRKY40)	Response to ABA, abiotic stress	Chen et al., 2010
AT3G46080	C2H2-type zinc finger family protein		
AT3G49620	DARK INDUCIBLE 11, DIN11	Sugar starvation	Fujiki et al., 2001
AT5G13080	WRKY DNA-BINDING PROTEIN 75 (WRKY75)	Pi starvation	Devaiah et al., 2007
Downregulated all strong mutants			
AT2G18300	HOMOLOG OF BEE2 INTERACTING WITH IBH 1 (HBI1)	Response to hormones, environmental signals, pathogen signals	Fan et al., 2014
AT3G58120	Member of the BZIP family of transcription factors (BZIP61)		

Table 2. Differentially Regulated Transcription Factors Shared between PR Mutants.
Genes were extracted from the top 50 up- and downregulated genes shared between all mutants (*hpr1*, *shm1*, *glyk1*, *pglp1*) or all strong mutants (*shm1*, *glyk1*, *pglp1*), which are listed in Supplemental Table 3.

PHOT2 expression was also significantly reduced by 70%–80% (Figure 4E).

Photorespiratory Mutants Are Confronted with Redox Stress upon LC Shift

Previous studies indicate a contribution of PR metabolism to the dissipation of excess excitation energy (Kozaki and Takeba, 1996; Takahashi and Badger, 2011). If PR played some role in the protection from photoinhibition and dissipation of excess excitation energy, we would expect enhanced oxidative stress after a shift to LC conditions in PR mutants. In the *hpr1* mutant, and especially pronounced in the strong mutants *shm1*, *glyk1*, and *pglp1*, we found an intense upregulation of stress indicators on both physiological and transcriptional levels upon LC shift. The photosynthetic electron transfer rate (ETR) decreased with increasing light intensity already under HC conditions (Supplemental Figure 3A), but more pronouncedly after the shift to LC conditions (Figure 5A). Reduced photosynthetic capacity was also reflected by enhanced non-photochemical quenching (NPQ) under both HC (Supplemental Figure 3B) and LC conditions (Figure 5B). Only the *pglp1* mutant was reduced in NPQ capacity after the LC shift (Figure 5B). Typical stress metabolites such as putrescine (Figure 5C) and proline (Supplemental Figure 3C) accumulated significantly in the *shm1* and *glyk1* mutants. If plants are stressed and challenged by high cellular redox status, they upregulate alternative electron valves for energy dissipation (Scheibe et al., 2005). Consistent with this, the expression of the alternative oxidases AOX1A and AOX1D was massively (20- to 40-fold for *AOX1A*, more than 1000-fold for *AOX1D*) enhanced on the transcriptional level in the strong PR mutants

(Figure 5D). For all parameters the *hpr1* mutant always showed an intermediate to WT-like behavior (Figure 5).

DISCUSSION

The dataset analyzed in this study strongly indicates that *Arabidopsis* WT plants respond in the short term to decreased external CO_2 concentrations on the physiological level but only to a limited degree on the transcriptional level. In total, just five genes showed significantly changed expression in WT plants (Table 1). The unchanged transcript levels of genes encoding enzymes involved in PR metabolism after a shift to LC conditions (Supplemental Table 4) indicate that the activity of PR metabolism is not controlled on the transcriptional level, at least not within the time frame analyzed in this study. Our results rather support the suggestion that regulation of PR flux occurs on the level of posttranslational modifications, such as phosphorylation of enzymes (Hodges et al., 2013). Elevated amounts of the PR signature intermediates glycolate, glycine, serine, and glycerate 1, 3, and 5 days after the shift to LC conditions (Figure 1 and Supplemental Figure 1) indicate an enhanced flux through this pathway. However, since PR runs at full capacity, WT plants do not show any of the stress symptoms we tested for (Figure 5). The only difference we observed was a change in the transpiration rate, which was elevated immediately after downshift and returned to pre-shift conditions after several days (Figure 4A). Higher transpiration means increased openness of stomata and was expected for the WT, since stomatal opening is induced within minutes of changing external CO_2 (Hu et al., 2010; Xue et al., 2011). The signal is routed through a phosphorylation cascade, which originates with carbonic anhydrases and is mediated through RESISTANT TO HIGH CARBON DIOXIDE 1 (RHC1), HIGH LEAF
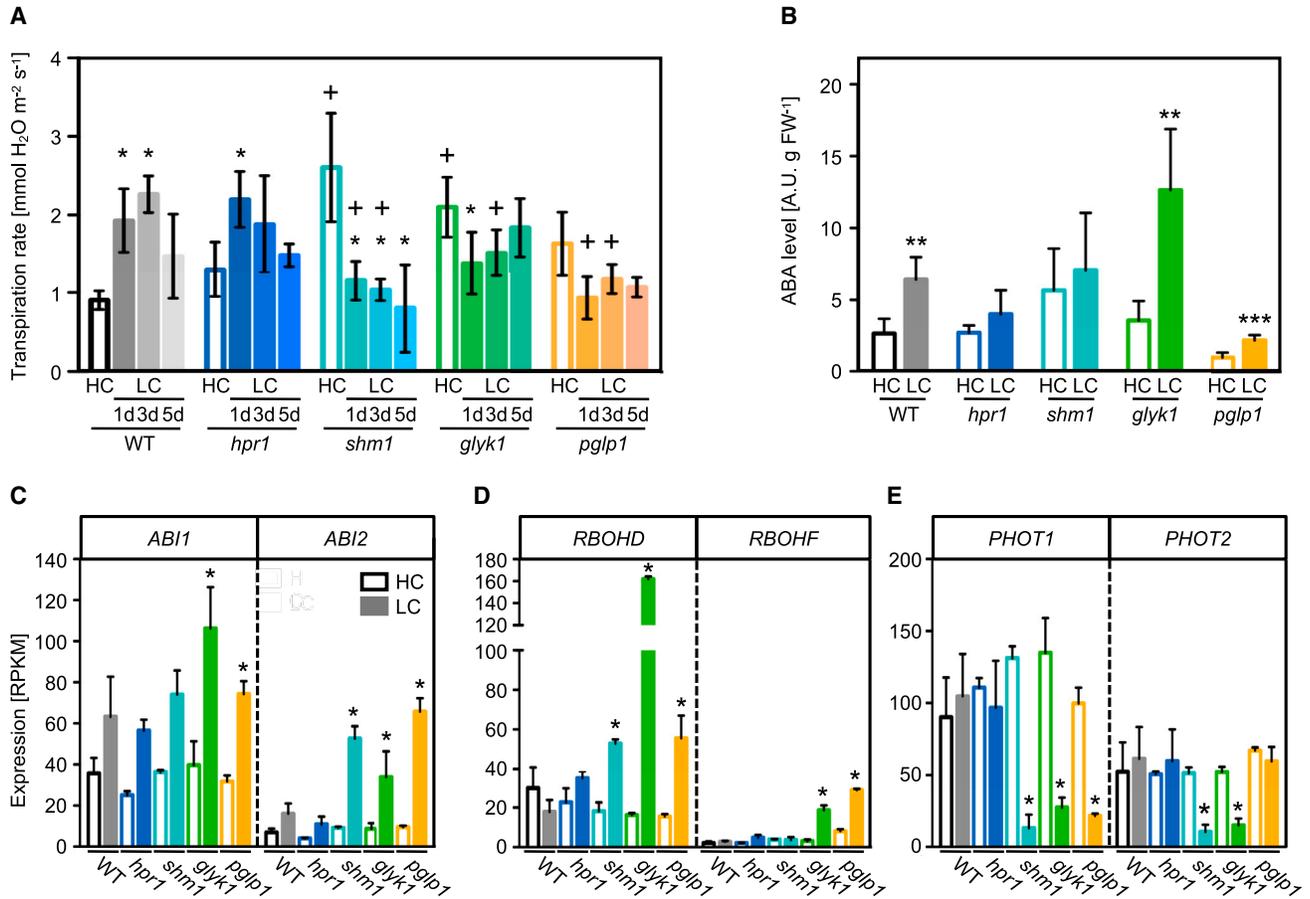
Figure 4. Response of Transpiration Rates and Regulatory Elements in Stomatal Aperture.

(A) Transpiration rates were measured before (HC) and after transfer to LC conditions (1, 3, and 5 days). Mean values ±SD (n = 4) are shown. Asterisks indicate significant changes according to the two-tailed Student's t-test (*P < 0.05) to the respective WT and mutant HC value. Plus signs (+) indicate significant changes to the corresponding WT value.

(B) Relative accumulation of ABA in leaves before (open bars) and 8 h after shift (filled bars) from HC to LC conditions. Given are means ± SD of five biological replicates. Asterisks indicate significant differences (P < 0.05) between HC and LC values. Significance was tested with the two-tailed Student's t-test. **P < 0.01; ***P < 0.001.

(C) Transcript abundance of the negative regulators in ABA-signaling *ABI1* and *ABI2* in leaves of WT and PR mutants under HC conditions and 8 h after shift to LC conditions.

(D) Transcript abundance of the respiratory burst oxidase proteins *RBOHD* and *RBOHF* in leaves of WT and PR mutants under HC conditions and 8 h after shift to LC conditions.

(E) Transcript abundance of the phototropins *PHOT1* and *PHOT2* in leaves of WT and PR mutants under HC conditions and 8 h after shift to LC conditions. Values in **(C)**, **(D)**, and **(E)** are presented as means of reads per kilobase of transcript per million reads mapped (RPKM) ± SD. Significant differences in transcript accumulation were tested with edgeR (Robinson et al., 2010) and are indicated with asterisks if q < 0.01.

TEMPERATURE 1 (HT1), and OPEN STOMATA 1 (OST1), and leads to stomatal closing if external CO_2 levels are raised and to stomatal opening if external CO_2 levels are lowered (Tian et al., 2015). Analyses of transcriptome data and transpiration rates both indicate that *Arabidopsis* CO_2 sensing returns to a new set point after about 5 days, at which time the ABA signal and the CO_2 signal are integrated in a way that prevents a drought response in leaves. Although, as a result of enhanced water loss ABA levels increased (Figure 4B) and a number of drought-stress-related genes, encoding anthocyanin biosynthetic pathway proteins, were induced (Table 1), the "open" signal affected by the reduction of CO_2 was in the short term stronger than the ABA-dependent "close" signal in WT plants. Long-term shift experiments for 3 and 5 days indicate that ABA-related signaling networks are induced at day 3 of a shift

from high CO_2 to ambient air and return to pre-shift conditions at day 5 (Queval et al., 2012), which coincides with a return to pre-shift transpiration rates after 5 days (Figure 4A).

The weak *hpr1* mutant behaved similarly to WT (Figure 4). The strong PR mutants *shm1*, *glyk1*, and *pglp1* showed paradoxical behavior with induction of stomatal closure upon a shift to LC conditions. Similar to WT they also accumulated ABA, whereas the increase was not significant in the *hpr1* and *shm1* mutants (Figure 4B). The GO term analysis indicates that these plants perceive themselves under pathogen attack as indicated by 23 out of 75 shared upregulated GO terms pertaining to innate immunity (Supplemental Table 2). The combined effect of signals is apparently stronger than the "open" signal affected by the reduction of CO_2, leading to rapidly reduced
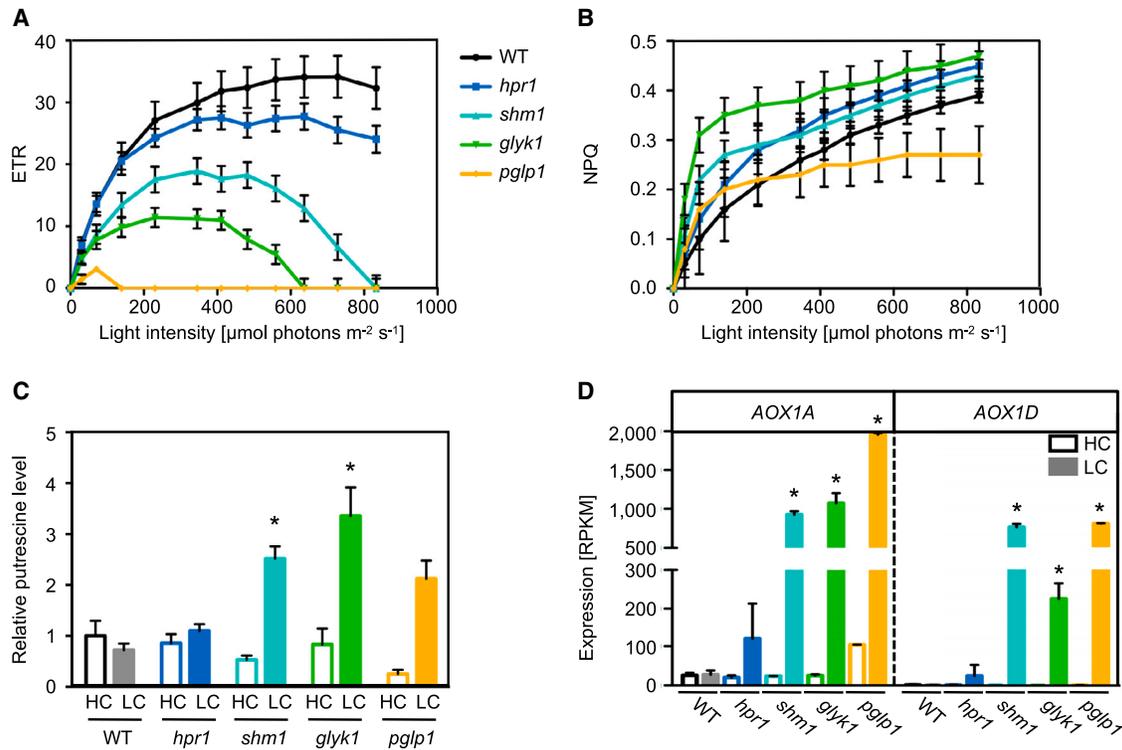
Figure 5. Stress Response of WT and PR Mutants after Shift from High CO₂ (HC, Open Bars) to Low CO₂ (LC) Conditions (Filled Bars).
(A) Effect of increasing light intensities on electron transfer rate (ETR).
(B) Effect of increasing light intensities on non-photochemical quenching (NPQ).
(C) Relative putrescine levels in leaves. Leaf material was harvested at the end of the day. Putrescine levels were normalized to the mean WT value under HC conditions.
(D) Accumulation of *AOX1A* and *AOX1D* transcripts.
Values are presented as means RPKM ± SD. Results are presented as means ± SD **(A, B, and D)** and means ± SE **(C)**, respectively. Asterisks indicate significant differences (*$P < 0.05$) between HC and LC values of the same plant line. Significant differences in transcript accumulation were tested with edgeR (Robinson et al., 2010) and are indicated with asterisks if $q < 0.01$ **(D)**.

transpiration rates in the strong mutants (Figure 4A). We also found in this study expression of several components of the guard cell signaling pathway specifically changed in the strong PR mutants upon the shift to LC conditions. On the one hand, both negative regulators of ABA-induced stomatal closure, ABI1 and ABI2 (Merlot et al., 2001), were upregulated (Figure 4C). On the other hand, the catalytic subunits of the guard cell localized NADPH oxidase RBOHF and RBOHD (Kwak et al., 2003) also were more strongly expressed under LC than HC conditions (Figure 4D). This oxidase generates ROS in guard cells and functions downstream of ABI1/ABI2 and OST1 as rate-limiting second messenger in ABA signaling, thus promoting closure of stomata (Kwak et al., 2003). Furthermore, transcript amounts of the BL mediators PHOT1 and PHOT2, which are central in controlling stomatal opening (Inoue et al., 2008), were considerably reduced in the strong mutants *shm1*, *glyk1*, and *pglp1* (Figure 4E). Therefore, we suggest that expression of *RBOHD*, *RBOHF*, *PHOT1*, and *PHOT2* in the light depends, directly or indirectly, on functional PR metabolism and contributes to the appropriate stomatal response to changing CO₂ availability. It must be noted that we did not determine the guard cell-specific transcriptome but the whole leaf accumulation of *PHOT1* and *PHOT2* transcripts. We can therefore only speculate on the reduced abundance of the BL receptors in the guard cells. In addition, it has been recently

shown that guard cell photosynthesis (Azoulay-Shemer et al., 2015) and mobilization of starch in guard cells (Prasch et al., 2015; Horrer et al., 2016) are both central in stomatal turgor generation and opening. Inhibition of photosynthesis in the strong PR mutants, as indicated by reduced ETR (Figure 5A), is likely associated with reduced accumulation of starch in stomatal guard cells (Figure 6). Reduced leaf starch contents were actually demonstrated for all mutants, *hpr1*, *shm1*, *glyk1*, and *pglp1*, 2 days after the shift from HC to LC conditions (Timm et al., 2012). This hypothesis is consistent with the reduced transpiration rates observed in the strong PR mutants after a shift to LC conditions (Figure 4A). Thus, a mutation in the PR pathway leaves the plant with multiple inputs on stomatal behavior. We interpret the reduced openness of stomata in the strong mutants as the sum output of signal integration at the stomata, which includes those by photosynthetic and starch status, CO₂, ABA, and innate immunity. The reduced expression of the phototropins PHOT1 and PHOT2 and the NADPH oxidase subunits RBOHF and RBOHD, together with the likely reduced starch accumulation in guard cells upon LC shift in the strong mutants, appears to be more dominant than the "open" signal. Therefore, despite impaired CO₂ fixation in *shm1*, *glyk1*, and *pglp1*, as indicated by reduced ETR (Figure 5A) and strongly elevated CO₂ compensation points (Timm et al., 2012), stomatal opening is not adjusted to
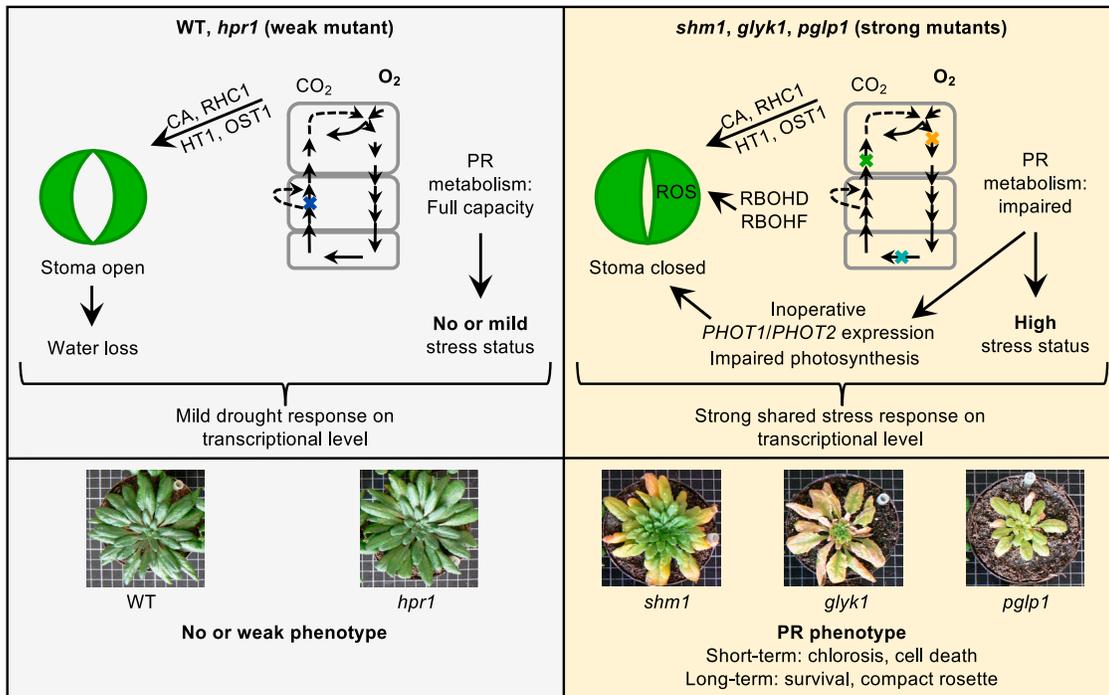
Figure 6. Role of PR Metabolism in Rapid Acclimation to Reduction in CO$_2$ Levels.
Reduction in external CO$_2$ concentrations leads to enhanced flux through the PR pathway. In WT and *hpr1* plants (left, gray box), PR metabolism has full or only slightly reduced capacity, and thus plants are not or mildly metabolically stressed. The reduction in CO$_2$ is perceived by carbonic anhydrases (CA) and initiates phosphorylation cascade, mediated through RESISTANT TO HIGH CARBON DIOXIDE 1 (RHC1), HIGH LEAF TEMPERATURE 1 (HT1), and OPEN STOMATA 1 (OST1). As a result, stomata open and plants lose water. Thus, on a transcriptional level plants show a mild drought response. Overall, WT and the weak mutant *hpr1* display no or only a weak phenotype. In the strong mutants *shm1*, *glyk1*, and *pglp1* (right, yellow box), PR metabolism is fully blocked. As a consequence, these mutants are highly stressed upon shift to reduced CO$_2$ concentrations. Metabolic and photosynthetic reactions are impaired and stress reactions induced. Although the stomatal CO$_2$ reception mechanism is operative, stomata close. Either the enhanced ROS production in guard cells by RBOHD/F and the reduced expression of phototropins PHOT1 and PHOT2 or impaired photosynthesis likely causes the stomatal closure. The high stress status brings about a strong transcriptional response, which leads to common reprogramming. For the strong mutants the ultimate outcome of reduction in CO$_2$ availability is chlorosis and cell death in source leaves in the short term. However, in the long term the reprogramming leads to survival of the *shm1* and *glyk1* plants in permissive light conditions as indicated by the appearance of young green leaves. The *pglp1* mutant does not survive long-term LC conditions. For a more detailed description, see text.

increase CO$_2$ input from the atmosphere. Moreover, in WT plants the same signals are integrated to mount an appropriate response to changing CO$_2$ conditions. However, since active PR allows unaffected photosynthesis (Figure 5A) and CO$_2$ fixation (Timm et al., 2012) after the shift to LC conditions, expression of PHOT1, PHOT2, RBOHF, and RBOHD (Figure 4D and 4E), and starch contents, remain stable. Thus, the sum output is the expected opening of stomata in the short term (Hu et al., 2010; Xue et al., 2011).

All mutants including the weak mutant *hpr1*, which carries only a partial block that can be circumvented by the action of two alternative HPR enzymes, HPR2 and HPR3 (Timm et al., 2011), showed a stronger transcriptional response compared with WT under LC conditions. Among the detected responses, GO terms related to transcriptional reprogramming, stress responses including redox stress, phytohormones, and cell death were elevated and some growth-related terms were reduced (Figure 3B and 3C). These stresses cannot be attributed to the absence of PR *per se*, since in HC none of these stresses were apparent in the transcriptome (Supplemental Table 4). Only the combination of limited CO$_2$ in

conjunction with impaired PR capacity invoked the response. A limitation in CO$_2$ results in acceptor limitation of photosynthesis and, hence, overreduction of the chloroplasts, which is exaggerated in the absence of a functional PR pathway (Igamberdiev et al., 2001; Scheibe and Dietz, 2012; Keech et al., 2016). To encounter the LC-induced redox stress, the strong mutants induced expression of several protective mechanisms, such as glutathione transferases with antioxidant function (Supplemental Table 3) and the mitochondrial electron valves AOX1A and AOX1D (Figure 5D), or enhanced NPQ (Figure 5B) to dissipate excess absorbed light energy. Thus, the analyses of redox-related processes indicated that overreduction of the chloroplast may at least be part of the signal leading to the transcriptional response, particularly since innate immunity is known to be signaled through ROS bursts (summarized in Göhre et al., 2012).

The three strong mutants *pglp1*, *shm1*, and *glyk1* showed a similar concerted response (Figure 3) independent of localization of the gene product and accumulation patterns of PR intermediates (Supplemental Table 1). Possibly this shared transcriptional pattern is at least partly modulated by the action

of specific transcription factors. Among the 50 most strongly changed and shared genes between the strong mutants were six transcription factors (Table 2), such as the central negative regulator of the ABA-signaling network, WRKY40 (Chen et al., 2010). With WRKY75 and DIN11 we could also identify transcription factors that are typically activated under starvation conditions. WRKY75 functions as a positive regulator during Pi starvation (Devaiah et al., 2007). DIN11 is strongly upregulated under sugar starvation conditions, i.e., when photosynthesis is inhibited (Fujiki et al., 2001). We suggest that the concerted action of all differentially regulated and shared transcription factors triggered major consistent reorganization within the strong mutants as indicated by the large share (>40%) of all differentially regulated genes in *shm1*, *glyk1*, and *pglp1* (Figure 3A). The strong mutants downregulated the central carbon metabolism, sulfur metabolism, Pi metabolism, and IPP biosynthesis related genes (Figure 3B), which indicated starvation and arrest of growth and shows the significant function of PR in metabolic repair. The signal produced by incomplete PR in conjunction with ambient CO_2 is thus strong enough to downregulate major growth processes. Presumably, metabolic resources become reallocated in the strong mutants to allow for investment into stress-related responses. This emergency strategy comes at the cost of growth. The observation that shoot apical meristem growth in seedlings of the PR mutants *shm1* and *bou*, which carries a defect in a mitochondrial transporter involved in PR, A BOUT DE SOUFFLE, is arrested under LC conditions (Eisenhut et al., 2013), is consistent with this hypothesis. Growth processes are also downregulated during the drought response characterized by limited CO_2 availability due to closed stomata, which explains the GO term enrichment with regard to water stress, which occurs in all mutants (Figure 3C). The strong mutants *pglp1*, *shm1*, and *glyk1* showed symptoms of carbon starvation also on a metabolic level, as indicated by enhanced breakdown of branched-chain amino acids (Supplemental Table 1; Araújo et al., 2010).

The emergency strategy indicated in the response (i.e., shutdown of growth, assimilation and major transcriptional investment pathways, breakdown of components), which serves plants well during temporary drought stress (Brilhaus et al., 2016), is not successful in the short term but can be in the long run. Although the block in PR leads to chlorosis and stunted to aborted growth in source leaves of the strong mutants (Figure 6) a few days after the shift from HC to LC conditions (Boldt et al., 2005; Voll et al., 2006; Schwarte and Bauwe, 2007; Timm et al., 2012), the strong mutants, except *pglp1* (Timm et al., 2012), survive after a long-term acclimation phase as long as light conditions are not prohibitive. The surviving *shm1* and to a minor degree also *glyk1* mutant plants acclimated after 2 weeks to LC conditions, displaying small green leaves and a compact rosette phenotype (Figure 6). For the *shm1* mutant it was demonstrated that the plant produces fertile seeds under these conditions (Timm et al., 2012). In this respect, the observation is interesting that the UDP-glucosyltransferase UGT74E2 was most strongly upregulated in all mutants (Supplemental Table 3). Its expression is H_2O_2 inducible and leads to indole-3-butyric acid-dependent morphological changes in plants. An overexpression line for UGT74E2 produced leaves with reduced area and was more tolerant toward water

stress (Tognetti et al., 2010). This compact rosette phenotype resembles the appearance of *shm1* and *glyk1* plants, 2 weeks after the shift from HC to LC conditions (Timm et al., 2012, Figure 6). Thus, the early upregulation of *UGT74E2* upon LC shift might be a keystone in improving the stress tolerance and survival of PR mutants in the long term in permissive light conditions. Prohibitive high light conditions may lead the plants into a vicious circle whereby ROS triggers an innate immunity response (Supplemental Table 2), which closes the stomata (Figure 4A), which in turn reduces long-term CO_2 availability, which more severely limits acceptor availability and thus triggers even higher ROS production. This circle may explain the longstanding observation that many PR mutants can be grown successfully, if very slowly, in low light conditions. It also implies that under natural conditions with fluctuating light intensities PR mutants would be outcompeted and not survive, respectively.

Since stomatal closure in the light as a consequence of a low water potential is associated with a strong reduction in leaf internal CO_2 (C_i) and hence depletion of the CBB cycle with acceptors, the rate of PR will be strongly increased under these conditions (decline of CO_2-to-O_2 ratio at the site of Rubisco). Thus, excess excitation energy will be immediately diverted toward driving the PR pathway, thereby providing an efficient means for photoprotection at the expense of oxidation of previously assimilated carbon. In the strong PR mutants, however, reduced external CO_2 concentration leads to a pronounced and rapid response of the transcriptome (Figures 2 and 3; Supplemental Figure 2). Hence, an intact PR pathway is required to maintain transcriptional homeostasis, possibly as discussed above by providing a means to dissipate excess excitation energy in the absence of sufficient CO_2 as an electron acceptor. This hypothesis is supported by previous findings that demonstrated rapid, O_2-dependent conversion of transitory starch into CBB-cycle intermediates upon withdrawal of CO_2 from the ambient air (Weise et al., 2006). This response was not observed in a pure nitrogen atmosphere, indicating that the oxygenation reaction of Rubisco is a key component of the energy dissipation reaction.

In summary, our results strongly support the hypothesis that PR safeguards photosynthetic metabolism from the consequences of Rubisco-catalyzed production of 2PG in the presence of O_2, and thus contributes to the rapid physiological acclimation during episodes of altered CO_2 availability to photosynthesis. If PR is impaired, both significant functions of the pathway, i.e., metabolic repair and photoprotection, are defunct. Accordingly, mutant plants are stressed upon LC shift and start a common transcriptional and physiological reprogramming for reallocation of resources from growth processes toward stress responses and enhanced energy dissipation.

METHODS

Plant Material and Growth Conditions

A. thaliana ecotype Columbia (Col-0) was used as WT reference during this study. T-DNA insertional lines for phosphoglycolate phosphatase (PGLP, *pglp1-1*), serine hydroxymethyltransferase (SHM, *shm1-2*), hydroxypyruvate reductase (HPR1, *hpr1-1*), and glycerate kinase (GLYK, *glyk1-1*) were obtained from the Nottingham Arabidopsis Stock Center and homozygous lines isolated as described previously (Boldt et al.,

2005; Voll et al., 2006; Schwarte and Bauwe, 2007; Timm et al., 2008). Prior cultivation seeds were surface sterilized with hypochloric acid, sown on soil, and incubated at 4°C for at least 2 days to break dormancy. Plants were grown in controlled environmental chambers (Percival; 10/14-h day/night cycle, 20/18°C, ~120 μmol m^{-2} s^{-1} irradiance, 10 000 ml l^{-1} CO$_2$, and 70% relative humidity) on a 4:1 mixture of soil (Type Mini Tray; Einheitserdewerk) and vermiculite, and regularly watered with 0.2% Wuxal liquid fertilizer (Aglukon). At growth stage 5.1 (Boyes et al., 2001) the HC-to-LC transition was carried out with reduction of the CO$_2$ concentration from high carbon (1%) to low carbon (0.038%) while all other growth parameters were kept constant.

Metabolite Analysis

Metabolite analysis was performed using 50 mg of fully expanded rosette leaves harvested from plants under HC and LC conditions (8 h after onset of illumination). Five biological replicates were analyzed. The extraction followed the protocol optimized for PR metabolites described in Pick et al. (2013). The derivatization and sample injection were performed exactly as described previously (Lisec et al., 2006). We used a GC-TOF-MS system consisting of an Agilent 7683B Series autosampler, an Agilent 7890A gas chromatograph system, and a LECO Pegasus HT-GC-TOF-MS system. Chromatograms and mass spectra were evaluated by Chroma TOF 4.24 (Leco) and TagFinder 4.0 for quantification and annotation of the peaks.

ABA Quantification

Ground frozen plant material (1 g, same sampling points as for metabolite analysis) was extracted in 10 ml of 80% acetonitrile containing 1% acetic acid and ^{6}D-ABA (1 ng/ml; Olchemin) overnight with shaking slowly at 4°C. The supernatant was obtained after centrifugation at 1700 g at 4°C for 10 min, and evaporated without heating until less than 7 ml. The pellet was re-suspended by mixing with the same extraction buffer (5 ml) and re-extracted for 3 h by shaking slowly at 4°C. The second supernatant was obtained after centrifugation at 1700 g at 4°C for 10 min. The combined extract fractions were evaporated until less than 7 ml, and 10 ml of ULC-MS grade water containing 1% aqueous acetic acid was added. After centrifugation, the supernatant was loaded onto a Strata-X 33u Polymeric Reversed Phase column (60 mg, 3 ml; Phenomenex) and prewashed/equilibrated consecutively with 3 ml of methanol and 1% acetic acid. After discarding the passed-through eluted fraction following sample loading, the column was washed with 1% aqueous acetic acid (1 ml). The ABA fraction was eluted with 80% methanol containing 1% acetic acid (2 × 500 μl) and evaporated without heating. The dried eluate was dissolved in 150 μl of 80% MeOH with 1% acetic acid. After centrifugation, the supernatant was subjected to liquid chromatography–tandem MS (MS/MS) in negative ion detection mode using a high-performance liquid chromatography (HPLC) Surveyor System coupled to an LTQ Linear ion trap electrospray ionization MS system (Thermo Finnigan). HPLC separation was performed with a Luna C18 column (2.0 × 150 mm, 3 μm particle size; Phenomenex) at a flow rate of 200 μl min^{-1} of 0.1% aqueous formic acid as solvent A and 0.1% acetic acid–acetonitrile as solvent B with linear gradient from 10% B to 30% B for 1 min, and to 50% B for 9 min. The initial condition was restored and washed (100% B) and allowed to equilibrate (10% B) for 2 min, respectively. The ABA-specific mass fragment peak (152.3–162.3 m/z) derived from MS/MS fragmentation (collision energy 70 eV) of the molecular parental ion peak ranging from 262.3 to 272.3 m/z was profiled. The obtained chromatogram was processed and peak area chosen using Quan Browser of Xcalibur software (Thermo Finnigan). Absolute concentration of endogenous ABA was estimated by the ratio to concentration of internal ^{6}D-ABA.

Gas Exchange and Chlorophyll a Fluorescence Measurements

Standard gas exchange measurements were performed on fully expanded leaves from plants in the second half of the light phase using a Licor-6400 (Licor, Lincoln, NE, USA) as described previously (Timm et al., 2012). Transpiration rates were determined under HC conditions and 1, 3, and 5 days after the transfer to normal air (LC). Relative ETR

and NPQ in response to increased light intensities were measured on an Imaging PAM (M-series, Walz) according to Schreiber et al. (1986) using plants grown under HC conditions to growth stage 5.1 (Boyes et al., 2001).

Genome-wide Gene Expression Analysis

For RNA isolation, leaf material was harvested 8 h after onset of illumination as pools from two independent plants per genotype in both HC and LC conditions, respectively. Total RNA extraction from liquid nitrogen frozen plant material was performed using the Nucleospin RNA plant kit (Macherey-Nagel) in conjunction with an additional DNAseI (Fermentas) treatment to remove genomic DNA contamination according to the manufacturers' protocols.

The quality of isolated RNA was checked with the Agilent 2100 bioanalyzer. cDNA libraries were prepared from 1 μg of RNA using the TruSeq RNA Sample Prep Kit v2 (Illumina, San Diego, USA). Sequencing was performed with the Illumina HiSeq2000 in the paired end mode. Illumina reads were processed and then mapped to the TAIR9 release of the A. thaliana genome (http://www.arabidopsis.org) using the CLC Genomics Workbench (CLC Bio, Aarhus, Denmark) with default parameters.

RNA-seq data were statistically evaluated using edgeR on raw read counts as implemented in Bioconductor (Robinson et al., 2010). Genes were called significantly differentially expressed if the false discovery rate (FDR) (q; Benjamini and Hochberg, 1995) was below 0.01. Reads per kilobase per million mapped reads (RPKM) were reported for all transcripts. RPKM values were averaged for the replicates of each condition and the log$_2$ fold changes between LC and HC values (i.e., LC/HC fold changes) were calculated by formally adding one read to all RPKM values to account for transcripts with no expression detected in one or more samples before fold-change calculation and logarithmic transformation ("pseudo-fold" changes; Bräutigam et al., 2011). This allowed us to keep genes with very low expression values under one of the conditions but markedly induced expression under the other condition in the datasets without significantly changing the actual logarithmized LC/HC ratios. The complete RNA-seq data of the experimental sets is provided in Supplemental Table 4.

Transcripts were annotated with descriptions from TAIR10 (Swarbreck et al., 2008). GO terms were downloaded for the TAIR10 annotation (www.arabidopsis.org). GO term enrichment for the ontology biological process for significantly up- and downregulated genes (FDR corrected q < 0.01) in each genotype was tested using TopGO in the R environment (Alexa and Rahnenfuhrer, 2010) with the node size cutoff at 10 nodes. Statistical significance was calculated with the classic Fisher's exact test (Fisher, 1922). The top 100 GO terms were reported in a table (Supplemental Table 2). For overlap calculations only GO terms with P values of <0.01 were considered (Supplemental Table 2).

ACCESSION NUMBERS

The read data have been submitted to the National Center for Biotechnology Information Gene Expression Omnibus under accession number GEO: GSE87329 (http://www.ncbi.nlm.nih.gov/geo/query/acc.cgi?acc=GSE87329).

SUPPLEMENTAL INFORMATION

Supplemental Information is available at Molecular Plant Online.

AUTHOR CONTRIBUTIONS

H.B., M.E., A.R.F., S.T., and A.P.M.W. designed the study. A.F., S.T., and T.T. carried out laboratory experiments. A.B. and M.E. carried out the

REFERENCES

Alexa, A., and Rahnenfuhrer, J. (2010). topGO: Enrichment Analysis for Gene Ontology. R Package Version 2.22.0.

Anderson, L.E. (1971). Chloroplast and cytoplasmic enzymes. II. Pea leaf triose phosphate isomerases. Biochim. Biophys. Acta **235**:237–244.

Araújo, W.L., Ishizaki, K., Nunes-Nesi, A., Larson, T.R., Tohge, T., Krahnert, I., Witt, S., Obata, T., Schauer, N., Graham, I.A., et al. (2010). Identification of the 2-hydroxyglutarate and isovaleryl-CoA dehydrogenases as alternative electron donors linking lysine catabolism to the electron transport chain of *Arabidopsis* mitochondria. Plant Cell **22**:1549–1563.

Azoulay-Shemer, T., Palomares, A., Bagheri, A., Israelsson-Nordstrom, M., Engineer, C., Bargmann, B., Stephan, A., and Schroeder, J.I. (2015). Guard cell photosynthesis is critical for stomatal turgor production, yet does not directly mediate CO₂- and ABA-induced stomatal closing. Plant J. **83**:567–581.

Bauwe, H., Hagemann, M., Kern, R., and Timm, S. (2012). Photorespiration has a dual origin and manifold links to central metabolism. Curr. Opin. Plant Biol. **15**:269–275.

Benjamini, Y., and Hochberg, Y. (1995). Controlling the false discovery rate: a practical and powerful approach to multiple testing. J. R. Stat. Soc. B **57**:289–300.

Boldt, R., Edner, C., Kolukisaoglu, U., Hagemann, M., Weckwerth, W., Wienkoop, S., Morgenthal, K., and Bauwe, H. (2005). D-GLYCERATE 3-KINASE, the last unknown enzyme in the photorespiratory cycle in *Arabidopsis*, belongs to a novel kinase family. Plant Cell **17**:2413–2420.

Boyes, D.C., Zayed, A.M., Ascenzi, R., McCaskill, A.J., Hoffman, N.E., Davis, K.R., and Görlach, J. (2001). Growth stage-based phenotypic analysis of *Arabidopsis*: a model for high throughput functional genomics in plants. Plant Cell **13**:1499–1510.

Bräutigam, A., Kajala, K., Wullenweber, J., Sommer, M., Gagneul, D., Weber, K.L., Carr, K.M., Gowik, U., Mass, J., Lercher, M.J., et al. (2011). An mRNA blueprint for C4 photosynthesis derived from comparative transcriptomics of closely related C3 and C4 species. Plant Physiol. **155**:142–156.

Brilhaus, D., Bräutigam, A., Mettler-Altmann, T., Winter, K., and Weber, A.P. (2016). Reversible burst of transcriptional changes during induction of crassulacean acid metabolism in *Talinum triangulare*. Plant Physiol. **170**:102–122.

Chen, H., Lai, Z., Shi, J., Xiao, Y., Chen, Z., and Xu, X. (2010). Roles of *Arabidopsis* WRKY18, WRKY40 and WRKY60 transcription factors in plant responses to abscisic acid and abiotic stress. BMC Plant Biol. **10**:281.

Devaiah, B.N., Karthikeyan, A.S., and Raghothama, K.G. (2007). WRKY75 transcription factor is a modulator of phosphate acquisition and root development in *Arabidopsis*. Plant Physiol. **143**:1789–1801.

Ding, Y., Liu, N., Virlouvet, L., Riethoven, J.J., Fromm, M., and Avramova, Z. (2013). Four distinct types of dehydration stress memory genes in *Arabidopsis thaliana*. BMC Plant Biol. **13**:229.

Eisenhut, M., Ruth, W., Haimovich, M., Bauwe, H., Kaplan, A., and Hagemann, M. (2008). The photorespiratory glycolate metabolism is essential for cyanobacteria and might have been conveyed endosymbiontically to plants. Proc. Natl. Acad. Sci. USA **105**:17199–17204.

Eisenhut, M., Planchais, S., Cabassa, C., Guivarc'h, A., Justin, A.M., Taconnat, L., Renou, J.P., Linka, M., Gagneul, D., Timm, S., et al. (2013). *Arabidopsis* A BOUT DE SOUFFLE is a putative mitochondrial transporter involved in photorespiratory metabolism and is required for meristem growth at ambient CO₂ levels. Plant J. **73**:836–849.

Engel, N., van den Daele, K., Kolukisaoglu, U., Morgenthal, K., Weckwerth, W., Pärnik, T., Keerberg, O., and Bauwe, H. (2007). Deletion of glycine decarboxylase in *Arabidopsis* is lethal under nonphotorespiratory conditions. Plant Physiol. **144**:1328–1335.

Falkowski, P., Scholes, R.J., Boyle, E., Canadell, J., Canfield, D., Elser, J., Gruber, N., Hibbard, K., Hogberg, P., Linder, S., et al. (2000). The global carbon cycle: a test of our knowledge of earth as a system. Science **290**:291–296.

Fan, M., Bai, M.Y., Kim, J.G., Wang, T., Oh, E., Chen, L., Park, C.H., Son, S.H., Kim, S.K., Mudgett, M.B., et al. (2014). The bHLH transcription factor HBI1 mediates the trade-off between growth and pathogen-associated molecular pattern-triggered immunity in *Arabidopsis*. Plant Cell **26**:828–841.

Fisher, R.A. (1922). On the interpretation of χ2 from contingency tables, and the calculation of P. J. R. Stat. Soc. **85**:87–94.

Fujiki, Y., Yoshikawa, Y., Sato, T., Inada, N., Ito, M., Nishida, I., and Watanabe, A. (2001). Dark-inducible genes from *Arabidopsis thaliana* are associated with leaf senescence and repressed by sugars. Physiol. Plant **111**:345–352.

Göhre, V., Jones, A.M., Sklenáø, J., Robatzek, S., and Weber, A.P. (2012). Molecular crosstalk between PAMP-triggered immunity and photosynthesis. Mol. Plant Microbe Interact. **25**:1083–1092.

Heber, U., and Krause, G.H. (1980). What is the physiological role of photorespiration? Trends Biochem. Sci. **5**:32–34.

Hodges, M., Jossier, M., Boex-Fontvieille, E., and Tcherkez, G. (2013). Protein phosphorylation and photorespiration. Plant Biol. **15**:694–706.

Horrer, D., Flütsch, S., Pazmino, D., Matthews, J.S., Thalmann, M., Nigro, A., Leonhardt, N., Lawson, T., and Santelia, D. (2016). Blue light induces a distinct starch degradation pathway in guard cells for stomatal opening. Curr. Biol. **26**:362–370.

Hu, H.H., Boisson-Dernier, A., Israelsson-Nordstrom, M., Bohmer, M., Xue, S.W., Ries, A., Godoski, J., Kuhn, J.M., and Schroeder, J.I. (2010). Carbonic anhydrases are upstream regulators of CO₂-controlled stomatal movements in guard cells. Nat. Cell Biol. **12**:87–93.

Huang, D., Wu, W., Abrams, S.R., and Cutler, A.J. (2008). The relationship of drought-related gene expression in *Arabidopsis thaliana* to hormonal and environmental factors. J. Exp. Bot. **59**:2991–3007.

Igamberdiev, A.U., Bykova, N.V., Lea, P.J., and Gardeström, P. (2001). The role of photorespiration in redox and energy balance of photosynthetic plant cells: a study with a barley mutant deficient in glycine decarboxylase. Physiol. Plant **111**:427–438.

Inoue, S., Kinoshita, T., Matsumoto, M., Nakayama, K.I., Doi, M., and Shimazaki, K. (2008). Blue light-induced autophosphorylation of phototropin is a primary step for signaling. Proc. Natl. Acad. Sci. USA **105**:5626–5631.

Keech, O., Gardeström, P., Kleczkowski, L.A., and Rouhier, N. (2016). The redox control of photorespiration: from biochemical and

physiological aspects to biotechnological considerations. Plant Cell Environ. http://dx.doi.org/10.1111/pce.12713.

Kelly, G.J., and Latzko, E. (1976). Inhibition of spinach-leaf phosphofructokinase by 2-phosphoglycollate. FEBS Lett. **68**:55–58.

Kinoshita, T., Doi, M., Suetsugu, N., Kagawa, T., Wada, M., and Shimazaki, K. (2001). phot1 and phot2 mediate blue light regulation of stomatal opening. Nature **414**:656–660.

Kollist, H., Nuhkat, M., and Roelfsema, M.R. (2014). Closing gaps: linking elements that control stomatal movement. New Phytol. **203**:44–62.

Kozaki, A., and Takeba, G. (1996). Photorespiration protects C3 plants from photooxidation. Nature **384**:557–560.

Kwak, J.M., Mori, I.C., Pei, Z.M., Leonhardt, N., Torres, M.A., Dangl, J.L., Bloom, R.E., Bodde, S., Jones, J.D., and Schroeder, J.I. (2003). NADPH oxidase AtrbohD and AtrbohF genes function in ROS-dependent ABA signaling in *Arabidopsis*. EMBO J. **22**:2623–2633.

Lisec, J., Schauer, N., Kopka, J., Willmitzer, L., and Fernie, A.R. (2006). Gas chromatography mass spectrometry-based metabolite profiling in plants. Nat. Protoc. **1**:387–396.

Marten, I., Deeken, R., Hedrich, R., and Roelfsema, M.R. (2010). Light-induced modification of plant plasma membrane ion transport. Plant Biol. **12**:64–79.

Merlot, S., Gosti, F., Guerrier, D., Vavasseur, A., and Giraudat, J. (2001). The ABI1 and ABI2 protein phosphatases 2C act in a negative feedback regulatory loop of the abscisic acid signalling pathway. Plant J. **25**:295–303.

Nakamura, Y., Kanakagiri, S., Van, K., He, W., and Spalding, M.H. (2005). Disruption of the glycolate dehydrogenase gene in the high-CO_2-requiring mutant HCR89 of *Chlamydomonas reinhardtii*. Can. J. Bot. **83**:820–833.

Nisbet, E.G., Grassineau, N.V., Howe, C.J., Abell, P.I., Regelous, M., and Nisbet, R.E.R. (2007). The age of Rubisco: the evolution of oxygenic photosynthesis. Geobiology **5**:311–335.

Norman, E.G., and Colman, B. (1991). Purification and characterization of phosphoglycolate phosphatase from the cyanobacterium *Coccochloris peniocystis*. Plant Physiol. **95**:693–698.

Osmond, C.B. (1981). Photorespiration and photoinhibition. Some implications for the energetics of photosynthesis. Biochim. Biophys. Acta **639**:77–98.

Pandey, G.K., Grant, J.J., Cheong, Y.H., Kim, B.G., Li, L., and Luan, S. (2005). ABR1, an APETALA2-domain transcription factor that functions as a repressor of ABA response in *Arabidopsis*. Plant Physiol. **139**:1185–1193.

Pick, T., Bräutigam, A., Schulz, M.A., Obata, T., Fernie, A.R., and Weber, A.P.M. (2013). PLGG1, a plastidic glycolate glycerate transporter, is required for photorespiration and defines a unique class of metabolite transporters. Proc. Natl. Acad. Sci. USA **110**:3185–3190.

Prasch, C.M., Ott, K.V., Bauer, H., Ache, P., Hedrich, R., and Sonnewald, U. (2015). β-Amylase1 mutant *Arabidopsis* plants show improved drought tolerance due to reduced starch breakdown in guard cells. J. Exp. Bot. **66**:6059–6067.

Queval, G., Neukermans, J., Vanderauwera, S., Van Breusegem, F., and Noctor, G. (2012). Day length is a key regulator of transcriptomic responses to both CO_2 and H_2O_2 in *Arabidopsis*. Plant Cell Environ. **35**:374–387.

Robinson, M.D., McCarthy, D.J., and Smyth, G.K. (2010). edgeR: a Bioconductor package for differential expression analysis of digital gene expression data. Bioinformatics **26**:139–140.

Scheibe, R., and Dietz, K.J. (2012). Reduction-oxidation network for flexible adjustment of cellular metabolism in photoautotrophic cells. Plant Cell Environ. **35**:202–216.

Scheibe, R., Backhausen, J.E., Emmerlich, V., and Holtgrefe, S. (2005). Strategies to maintain redox homeostasis during photosynthesis under changing conditions. J. Exp. Bot. **56**:1481–1489.

Schreiber, U., Schliwa, U., and Bilger, W. (1986). Continuous recording of photochemical and nonphotochemical chlorophyll fluorescence quenching with a new type of modulation fluorometer. Photosynth. Res. **10**:51–62.

Schwarte, S., and Bauwe, H. (2007). Identification of the photorespiratory 2-phosphoglycolate phosphatase, PGLP1, in *Arabidopsis*. Plant Physiol. **144**:1580–1586.

Shimazaki, K., Doi, M., Assmann, S.M., and Kinoshita, T. (2007). Light regulation of stomatal movement. Annu. Rev. Plant Biol. **58**:219–224.

Somerville, C.R. (2001). An early *Arabidopsis* demonstration. Resolving a few issues concerning photorespiration. Plant Physiol. **125**:20–24.

Somerville, C.R., and Ogren, W.L. (1979). A phosphoglycolate phosphatase-deficient mutant of *Arabidopsis*. Nature **280**:833–836.

Swarbreck, D., Wilks, C., Lamesch, P., Berardini, T.Z., Garcia-Hernandez, M., Foerster, H., Li, D., Meyer, T., Muller, R., Ploetz, L., et al. (2008). The *Arabidopsis* Information Resource (TAIR): gene structure and function annotation. Nucleic Acids Res. **36**:D1009–D1014.

Szecowka, M., Heise, R., Tohge, T., Nunes-Nesi, A., Vosloh, D., Huege, J., Feil, R., Lunn, J., Nikoloski, Z., Stitt, M., et al. (2013). Metabolic fluxes in an illuminated *Arabidopsis* rosette. Plant Cell **25**:694–714.

Takahashi, S., and Badger, M.R. (2011). Photoprotection in plants: a new light on photosystem II damage. Trends Plant Sci. **16**:53–60.

Takahashi, S., Bauwe, H., and Badger, M. (2007). Impairment of the photorespiratory pathway accelerates photoinhibition of photosystem II by suppression of repair but not acceleration of damage processes in *Arabidopsis*. Plant Physiol. **144**:487–494.

Tian, W., Hou, C., Ren, Z., Pan, Y., Jia, J., Zhang, H., Bai, F., Zhang, P., Zhu, H., He, Y., et al. (2015). A molecular pathway for CO_2 response in *Arabidopsis* guard cells. Nat. Commun. **6**:6057.

Timm, S., and Bauwe, H. (2013). The variety of photorespiratory phenotypes—employing the current status for future research directions on photorespiration. Plant Biol. **15**:737–747.

Timm, S., Nunes-Nesi, A., Pärnik, T., Morgenthal, K., Wienkoop, S., Keerberg, O., Weckwerth, W., Kleczkowski, L.A., Fernie, A.R., and Bauwe, H. (2008). A cytosolic pathway for the conversion of hydroxypyruvate to glycerate during photorespiration in *Arabidopsis*. Plant Cell **20**:2848–2859.

Timm, S., Florian, A., Jahnke, K., Nunes-Nesi, A., Fernie, A.R., and Bauwe, H. (2011). The hydroxypyruvate-reducing system in *Arabidopsis thaliana*—multiple enzymes for the same end. Plant Physiol. **155**:694–705.

Timm, S., Mielewczik, M., Florian, A., Frankenbach, S., Dreissen, A., Hocken, N., Fernie, A.R., Walter, A., and Bauwe, H. (2012). High-to-low CO_2 acclimation reveals plasticity of the photorespiratory pathway and indicates regulatory links to cellular metabolism of *Arabidopsis*. PLoS One **7**:e42809.

Tognetti, V.B., Van Aken, O., Morreel, K., Vandenbroucke, K., van de Cotte, B., De Clercq, I., Chiwocha, S., Fenske, R., Prinsen, E., Boerjan, W., et al. (2010). Perturbation of indole-3-butyric acid homeostasis by the UDP-glucosyltransferase UGT74E2 modulates *Arabidopsis* architecture and water stress tolerance. Plant Cell **22**:2660–2679.

Voll, L.M., Jamai, A., Renné, P., Voll, H., McClung, C.R., and Weber, A.P. (2006). The photorespiratory *Arabidopsis shm1* mutant is deficient in SHM1. Plant Physiol. **140**:59–66.

Voss, I., Sunil, B., Scheibe, R., and Raghavendra, A.S. (2013). Emerging concept for the role of photorespiration as an important part of abiotic stress response. Plant Biol. **15**:713–722.

Weise, S.E., Schrader, S.M., Kleinbeck, K.R., and Sharkey, T.D. (2006). Carbon balance and circadian regulation of hydrolytic and phosphorolytic breakdown of transitory starch. Plant Physiol. **141**:879–886.

Xue, S.W., Hu, H.H., Ries, A., Merilo, E., Kollist, H., and Schroeder, J.I. (2011). Central functions of bicarbonate in S-type anion channel activation and OST1 protein kinase in CO_2 signal transduction in guard cell. EMBO J. **30**:1645–1658.

Zhu, Q., Zhang, J., Gao, X., Tong, J., Xiao, L., Li, W., and Zhang, H. (2010). The *Arabidopsis* AP2/ERF transcription factor RAP2.6 participates in ABA, salt and osmotic stress responses. Gene **457**:1–12.